https://doi.org/10.1016/j.fuel.2021.121015

Innovative Application of Waste Polyethylene Terephthalate (PET) Derived Additive as An Antistripping Agent for Asphalt Mixture: Experimental Investigation and Molecular Dynamics Simulation

Rui Li [a], Zhen Leng [a*], Jun Yang [c], Guoyang Lu [a], Man Huang [b], Jingting Lan [a], Hongliang Zhang [b], Yawei Bai [d], Zejiao Dong [e]

[a] Department of Civil and Environmental Engineering, The Hong Kong Polytechnic University, Hong Kong SAR, China

[b] Key Laboratory for Special Area Highway Engineering of Ministry of Education, Chang'an University, Xi'an, China

[c] School of Transportation, Southeast University, Nanjing, China

[d] Henan Province Highway Management Center of Toll and Loan, Zhengzhou, China

[e] School of Transportation Science and Engineering, Harbin Institute of Technology, Harbin, China

*** Corresponding Author.**

E-mail: zhen.leng@polyu.edu.hk

Abstract: Moisture-induced damage represents one of the major challenges to the durability of asphalt pavement, which may lead to various premature distresses, such as cracking, ravelling and potholes. To reduce the moisture-induced damages, antistripping agents have been commonly used in asphalt mixtures. On the other hand, the fast-growing waste polyethylene terephthalate (PET) from the end-of-life plastic products poses a serious problem to the environment. How to recycle and reuse the waste PET is becoming a major concern. This study aims to develop a value-added recycling approach of reusing waste PET as an antistripping agent for asphalt mixture. To achieve this objective, waste PET was first collected and went through an aminolysis reaction to yield the amine-based PET additive, which was used to modify bitumen. The infrared spectrum of the PET additive was then characterized, followed by the evaluation of moisture susceptibility through the boiling test and indirect tensile strength (ITS) test. In addition, molecular dynamics (MD) simulation was conducted to analyze the effect of the PET additive on the density and the cohesive energy density (CED) of the binder, and the interface bonding between binder and aggregate at the molecular level. The results from both experiments and MD simulation consistently indicate that the waste PET derived additive can effectively increase the resistance to moisture-induced damage of asphalt mixture.

Keywords: Polyethylene terephthalate (PET); Moisture damage; Adhesion; Antistripping; Molecular dynamics simulation

1. Introduction

Asphalt pavements are subjected to various damages caused by vehicle loads and environmental effects, among which, the moisture-induced damage is recognized as one of the most important factors affecting the durability of pavements [1]. Moisture-induced damage often leads to stripping

of asphalt mixture [2], as a result of the loss of interface adhesion between bitumen and aggregate or the reduction of cohesion within asphalt mastic under the effect of water [3]. It has been reported that moisture-induced damage could also accelerate premature failures of pavements such as cracking, ravelling and potholes [4, 5]. The potential of moisture-induced damage is largely dependent on the physico-chemical properties of bitumen and aggregate [6]. As most of the mineral aggregates are hydrophilic, their affinity to water normally exceeds that to bitumen [7-9]. Thus, the binder film around aggregate is prone to be replaced by water as water diffuses to the asphalt-aggregate interface.

To reduce the moisture susceptibility, additives such as liquid fatty amines and hydrated lime have been applied as the antistripping agents for hot-mix asphalt [10, 11]. Due to the convenience of application, liquid amines are more favored [12]. Various studies have been conducted to investigate the effect of amine-based antistripping agents on moisture-induced damages of asphalt mixtures, and the results proved that these antistripping agents can effectively reduce the moisture susceptibility [13-15].

Polyethylene terephthalate (PET) is a plastic polymer, which is commonly used to make plastic bottles. The fast-growing consumption of plastic bottles has created a serious environmental problem in recent years. As the polymeric PET bottles are not bio-degradable, how to recycle and reuse the waste PET bottles poses a major challenge to environment. The application of waste PET in asphalt mixture provides a possible solution to reuse this waste material. Due to the fact that the melting point (~250℃) of PET is very high [16], it is not feasible to prepare a homogeneous PET modified bitumen with the wet process. Instead, most previous studies used the dry process to prepare PET modified asphalt mixture, i.e., the PET flakes were added into asphalt mixture directly during the mixing of asphalt binder and aggregate. It was found that PET increased the fatigue life

of asphalt mixtures to some extent, while the resistance to moisture damage decreased [17-19], which was mainly due to the poor adhesion between asphalt binder and the PET flakes. On the other hand, chemical treatment of waste PET for the preparation of PET derived additive has been found to be a promising alternative to the aforementioned dry process [20-22]. Recently, the aminolysis product of waste PET was employed to modify bitumen by Leng, et al. [20, 23], and the results highlighted that the PET derived additive significantly increased the adhesion between asphalt binder and aggregate, therefore reducing the moisture-induced damage. Nevertheless, the adhesion mechanism between the PET additive modified asphalt binder and aggregate has not been fully understood yet. Previous studies have indicated that molecular dynamics (MD) simulation can provide fundamental insights in understanding the interface adhesion between binder and aggregate from the molecular or atomic level [24, 25]. It is therefore meaningful to explore the interface performance between the PET additive modified binder and aggregate employing the MD simulation.

MD simulation has been widely used to study various properties of asphalt binder and mixture, including the density, cohesion, and particularly adhesion properties [25-28]. Xu and Wang [24] investigated the interface adhesion between binder and aggregate using the bond energy parameters in both dry and wet conditions obtained from MD simulation. Their results indicated that both the aggregate and binder types affect the interfacial adhesion. The study by Yao, et al. [29] indicated that aggregate tends to affiliate more to water than bitumen, as the adhesion energy between aggregate and water is larger than that between aggregate and bitumen binder. Zhang, et al. [21] recently verified that the glycolysis treated PET can improve the adhesion between binder and aggregate through MD simulation. The aminolysis product of waste PET showed strong antistripping ability in our previous study [20], and the MD simulation can be applied to provide

more in-depth understanding of the effect of PET additive on the interface adhesion between binder and aggregate from the molecular perspective.

The main objective of this research is to investigate the antistripping performance of the PET derived additive in asphalt mixture through combined experimental investigation and MD simulation. To achieve this objective, the aminolysis treated waste PET additive was first used to produce modified bitumen. The moisture susceptibilities of the PET additive modified bitumen and asphalt mixture were then evaluated experimentally through the boiling test and indirect tensile strength (ITS) test. Finally, the MD simulation was implemented to evaluate the density and cohesive energy density (CED) of the PET additive modified binder, and the adhesion between the binder and aggregate in both dry and wet conditions.

2. Materials and methods

2.1 Materials

In this study, the PET additive was obtained through aminolysis treatment of waste PET. Waste PET bottles were collected after proper identification. Triethylenetetramine (TETA) was purchased from Sigma-Aldrich. Neat bitumen with a penetration grade of 60/70 (Pen 60/70) was used, and its basic properties are presented in Table 1. Crushed granite aggregate and mineral filler were obtained from a local supplier. The aggregate gradation for WC10 (a dense-graded wearing course mixture with a nominal maximum aggregate size of 10mm commonly used in Hong Kong) was used as shown in Figure 1.

Table 1. Basic properties of bitumen

Penetration (25 °C, 0.1 mm)	Softening point (°C)	Viscosity at 135 °C (mPa·s)

64.5	48.5	477.5

104

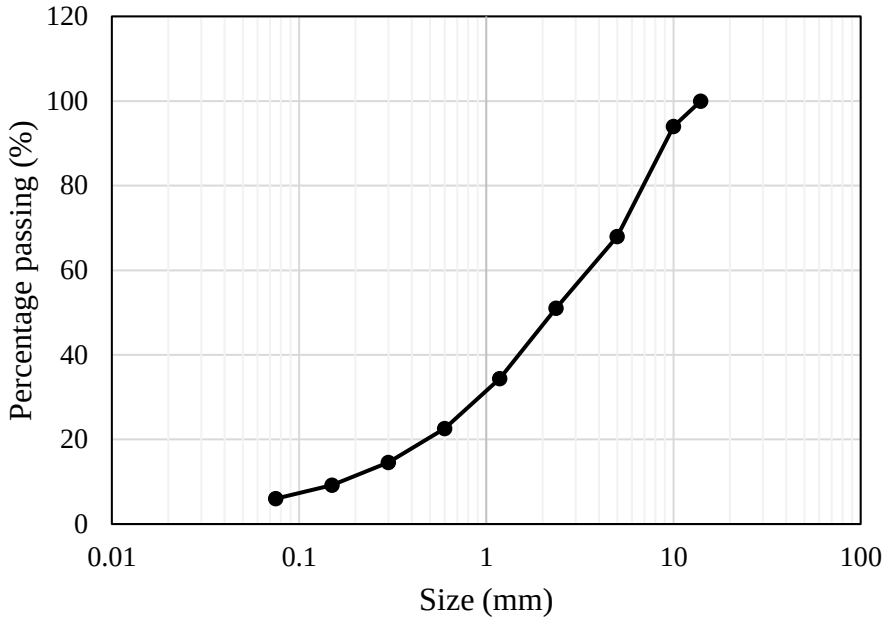

105

106 **Figure 1.** Gradation of aggregate

107 **2.2 Aminolysis of waste PET**

108 The aminolysis of waste PET was carried out following the procedure as presented in Figure 2.
109 Prior to the aminolysis treatment, the PET bottles were first cleaned with normal detergent and
110 then cut into small flakes, which were subsequently dried in an oven at 80 °C for 2 h. A 500 ml
111 four-necked round flask equipped with a stirrer, reflux condenser and nitrogen gas, was heated in
112 an oil bath and charged with waste PET flakes and TETA. The weight ratio of PET to TETA was
113 1:2 based on a previous study [20]. The aminolysis reaction of PET was conducted at around
114 140 °C for 2 h. After this treatment, the homogeneous product was cooled down to room
115 temperature and then filtrated with deionized water for at least three times to remove the excess
116 TETA and by-products (ethylene glycol. Finally, the substance remaining on the filter paper was

collected and dried in an oven at 60 °C for 2-3 h to obtain the PET additive. Figure 3 shows the chemical reaction between PET and TETA during aminolysis.

(a) (b) (c) (d)

Figure 2. Aminolysis treatment of waste PET bottles to produce PET additive: (a) waste PET bottles, (b) PET flakes, (c) aminolysis reaction, and (d) the prepared PET additive ready for use.

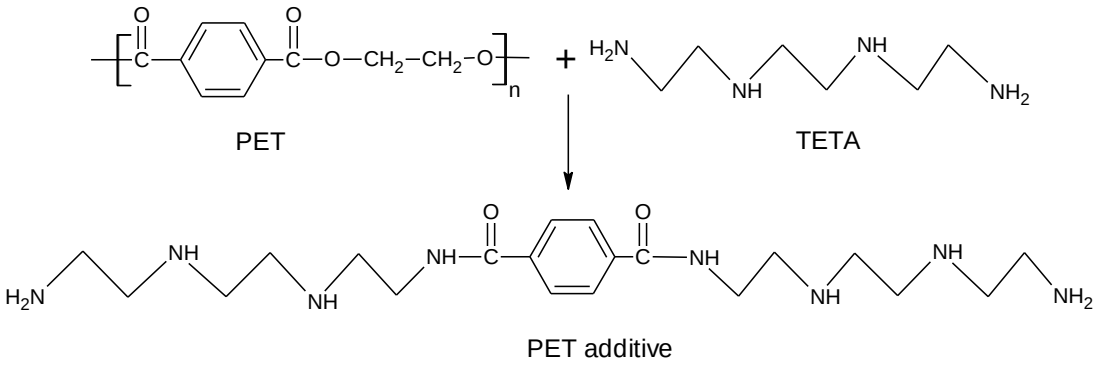

Figure 3. Aminolysis reaction of PET. The PET flakes reacted with TETA at a temperature of 140 °C for 2 h to prepare the PET derived additive.

2.3 Preparation of PET additive modified asphalt binder

To prepare the PET additive modified asphalt binder, approximately 500 g of bitumen was first heated to fluid condition at 150 °C. The pre-weighted PET additive was then added into the binder and stirred at a speed of 500 rpm for 1 h. PET modified binders with two different weight percentages of PET additive, 1wt% and 3wt% based on bitumen, were prepared and denoted as PETB-1 and PETB-3, respectively. The neat binder Pen 60/70 without PET additive was used for comparison.

2.4 Experimental characterizations

Infrared spectra measurements were performed using a Bruker Tensor II Fourier Transform Infrared (FT-IR) spectrometer. The IR spectrum of PET additive was measured from 600 cm^{-1} to 4,000 cm^{-1} with a resolution of 4 cm^{-1}.

The conventional bitumen binder tests of penetration at 25 °C, softening point and rotational viscosity from 120 °C to 175 °C were carried out following ASTM D5, D36 and D4402, respectively.

The adhesion between bitumen and aggregates was evaluated through the boiling water test in accordance with ASTM D3625. Around 400 g of coarse aggregates with the size of 5-10 mm were mixed with bitumen for the boiling test. To prepare a layer of binder film with a thickness of 8-10 microns, 2wt% of binder based on aggregates was applied [6, 30]. The mixtures were subsequently boiled for 10 min in a beaker. Finally, the boiled mixtures were scanned with a normal office scanner to obtain the images.

The moisture susceptibility of PET modified asphalt mixture was then evaluated through indirect tensile strength (ITS) test at 20 °C according to ASTM D4867. The compacted asphalt mixture with an air void of 6-8% was first prepared with the Marshall compactor. Two groups of specimens were fabricated and subjected to dry and wet conditioning, respectively. The dry group specimens were conditioned at room temperature (23 ± 0.5 °C) for 24 h, and the wet group specimens were immersed in the 60 °C water for another 24 h following the dry conditioning procedure. The ITS tests for the two groups of specimens were then conducted, and the tensile strength ratio (TSR) between the wet conditioned strength and the dry strength were then calculated.

2.5. Molecular dynamics simulation

2.5.1 Molecular models

Bitumen, a byproduct originating from the crude oil distillation, is composed of various hydrocarbons. The main components of bitumen can be divided into asphaltenes, resins, aromatics, and saturates, based on their polarity and aromaticity [31]. Bitumen constitutes a wide range of different molecules whose structures are still not totally clear, which makes it challenging to study this material using MD simulation. Considering the complexity of bitumen, it is almost impossible to construct a molecular model that represents its accurate composition at present. Instead, simplified models that are composed of 3-12 representative molecule types were commonly used [32, 33]. Since the objective of this study is to evaluate the effect of PET additive on the antistripping performance of the binder, the three-component bitumen model [34] was adopted for its simplicity. The three components are asphaltene ($C_{64}H_{52}S_2$), 1,7-Dimethylnaphthalene ($C_{12}H_{22}$), and n-docosane (n-$C_{22}H_{46}$), which represent asphaltene, naphthene aromatic and saturate, respectively. Figure 4 illustrates the molecular structures of the three-component bitumen model and that of the PET additive.

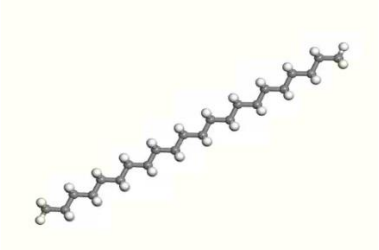

(a) n-docosane (n-$C_{22}H_{46}$)

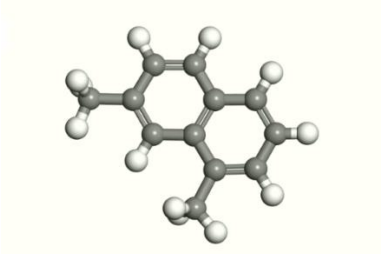

(b) 1,7-dimethylnaphthalene ($C_{12}H_{12}$)

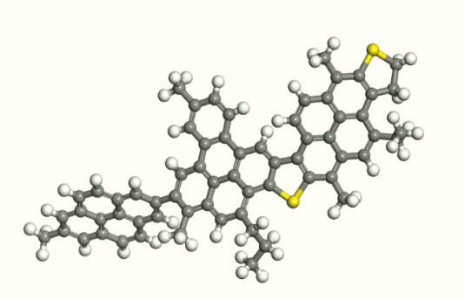

(c) Asphaltene ($C_{64}H_{52}S_2$)

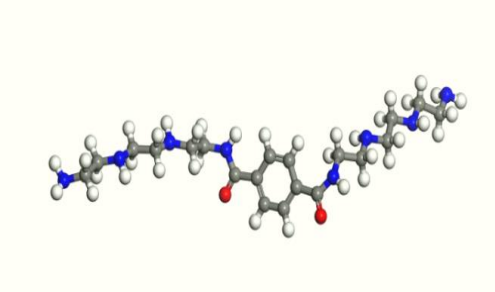

(d) PET additive ($C_{20}H_{38}O_2N_8$)

Figure 4. Molecular structures of (a) n-docosane (n-$C_{22}H_{46}$), (b) 1,7-dimethylnaphthalene ($C_{12}H_{12}$), (c) Asphaltene ($C_{64}H_{52}S_2$), and (d) PET additive ($C_{20}H_{38}O_2N_8$). Note that the grey atoms represent C, the white atoms represent H, the yellow atoms represent S, the blue atoms represent N, and the red atoms represent O. (Please refer to the online version for the colors of the atoms)

2.5.2 Bulk binder model

The molecular compositions of the neat bitumen and PET modified bitumen (PETB) are presented in Table 2, the number of molecules were selected based on previous studies [34-36]. The mass fractions of asphaltene, 1,7-dimethylnaphthalene, and n-docosane in the neat bitumen are 20.7wt%, 19.7wt%, and 59.6wt%, respectively. According to the experiment results, 1wt% of PET additive could already achieve good antistripping performance, thus only 1 PET additive molecule was added to construct the PETB model, which corresponds to 1.97wt% of PET additive based on bitumen.

Table 2. Molecular compositions of binder

Sample-ID	Asphaltene ($C_{64}H_{52}S_2$)	1,7-dimethylnaphthalene ($C_{12}H_{12}$)	n-docosane (n-$C_{22}H_{46}$)	PET additive	PET additive wt%
Neat bitumen	5	27	41	/	/
PETB	5	27	41	1	1.97

In this study, the commercial software BIOVIA Materials Studio was used to perform the molecular dynamics (MD) simulation. The COMPASS (Condensed-phase Optimized Molecular Potentials for Atomistic Simulation Studies) force field, developed using *ab initio* and empirical parameterization techniques by Sun [37], has been commonly applied to describe the interactions of bituminous materials [38-40]. The Nose-Hoover-Langevin (NHL) thermostat and the Andersen barostat were employed throughout the simulation to control the temperature and pressure, respectively. A cut-off distance of 15.5 Å was used to speed up the computation. To build the bulk binder model, an amorphous cell with an initial density of 0.1 g/cm^3 in 3D periodical condition was constructed first. After a geometry optimization process using the steepest descent algorithm, the system was then annealed for five cycles from 300 K to 500 K. Following a pre-equilibrium run for 100 ps with a time step of 1 fs under canonical ensemble (NVT), the system went through a 200 ps relaxation and shrank to a stable state with the isothermal-isobaric (NPT) ensemble. Finally, another simulation run of 100 ps was performed with the canonical ensemble to further equilibrate the system (Figure 5). Unless additionally stated, the temperature and pressure were set as 298 K and 0.0001 GPa (1atm), respectively, during the simulation.

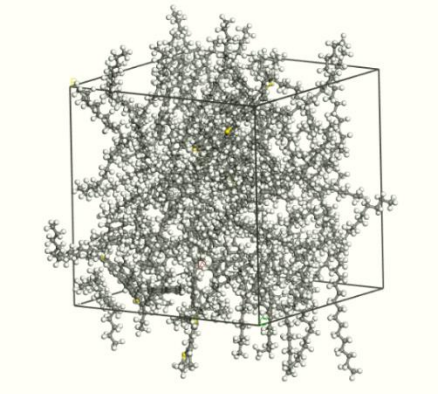

Figure 5. Bulk bitumen model after equilibrium. A total of 73 molecules are included, containing 4026 atoms. (Please refer to the online version for the colors of the atoms)

2.5.3 Aggregate-bitumen interface model

Silica (SiO_2), commonly used in the aggregate model for asphalt mixture simulation, was adopted in this study to represent aggregate. A unit silica model with the lattice parameters of a = b = 4.91 Å, c = 5.402 Å, α = β = 90 °, and γ = 120° normally applied to build the siliceous aggregate model was selected in this study. The unit silica model was first cleaved in the (1 0 0) surface, which was then used to build a supercell with the size of 35Å×35Å×23Å (Figure 6). Geometry optimization of the supercell was performed before constructing the aggregate-bitumen interface. It was reported that the surface silicone atoms in siliceous aggregate are attached with hydroxyl groups (-OH) [41]. According to previous studies, the density of the surface hydroxyl groups was set as 4.56 OH/nm^2 [42, 43].

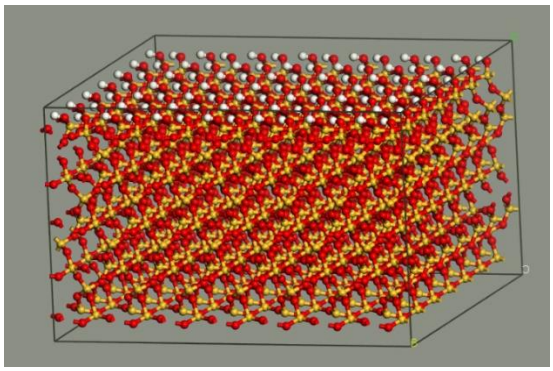

Figure 6. Supercell of SiO_2.The size of the SiO_2 supercell is 35Å×35Å×23Å, and the surface silicon atoms are attached with hydroxyl groups -OH.

The aggregate-bitumen interface was built by placing a confined bitumen layer on top of the aggregate layer. To avoid the interaction across the mirror image in the z-direction, a vacuum layer of 30 Å was added above the bitumen layer. After geometry optimization, the interface was equilibrated at the canonical ensemble for 200 ps. Figure 7 shows the initial configuration and the equilibrated configuration of the interface model in dry condition.

To evaluate the influence of water on the properties of binder-aggregate interface, 200 water molecules were placed between the aggregate layer and bitumen layer, based on the experience of the previous studies [24, 44]. The interface model with water was then subjected to the same equilibrium procedure as described for the interface model without water. Figure 8 shows the initial configuration and the equilibrated configuration of the interface model in wet condition.

(a) (b)

Figure 7. Initial configuration (a) and equilibrated configuration (b) of the interface model in dry condition. A vacuum layer of Å was placed on top of the bitumen layer to avoid interaction across the mirror image.

(a) (b)

Figure 8. Initial configuration (a) and equilibrated configuration (b) of the interface model in wet condition. 200 water molecules were inserted between the aggregate layer and bitumen layer.

3. Experimental results

3.1 FT-IR test

Figure 9 illustrates the FT-IR spectrum of the PET additive. It can be observed that the distinct peak at 1,720 cm^{-1} corresponding to the carbonyl (-C=O) stretching vibration of the ester group in PET molecules disappeared, while the two peaks at 1,636 cm^{-1} and 1,547 cm^{-1} corresponding to the characteristic carbonyl (-C=O) stretching vibration and N-H bending vibration of the amide group in PET additive, respectively, emerged. In addition, the peak at 3,320 cm^{-1} attributed to the stretching vibration of the N-H in the amine group also showed up. This result indicated the successful aminolysis of the waste PET by TETA.

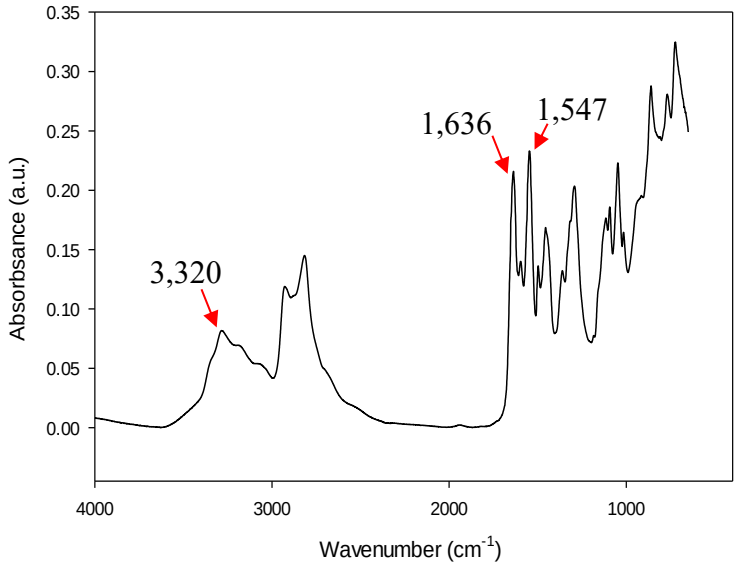

Figure 9. FT-IR spectrum of PET additive. The peaks at 1,636 cm^{-1} and 1,547 cm^{-1} were attributed to the carbonyl (-C=O) stretching vibration and N-H bending vibration of the amide group in PET additive, respectively, and the peak at 3,320 cm^{-1} corresponds to the stretching vibration of the N-H in amine group.

3.2 Basic properties of binders

Table 3 compares the values of penetration and softening point of the base bitumen and the PET additive modified bitumens. It can be seen that penetration decreased while the softening point increased slightly with the incorporation of the PET additive. In addition, the binders with 1wt% and 3wt% of PET additive resulted similar values of penetration and softening point.

Table 3. Penetration and softening point of binders

Sample-ID	Penetration (25 °C, 0.1 mm)	Softening point (°C)
Pen 60/70	64.5	48.5
PETB-1	53.6	50.0
PETB-3	53.2	49.6

The viscosity of PET additive modified binders as a function of temperature from 120-175℃ is shown in Figure 10. It is observed that the viscosity increased a little bit with addition of PET additive at lower temperature (120 ℃). With the increase of temperature, the viscosity become similar for all the binders. In fact, the viscosity did not show much difference with temperatures above 150 ℃. The underlying reason is that the PET additive may form a crystal at ambient temperature [23], due to the linearity of its molecule structure and the presence of amino groups that leads to hydrogen bonds between the molecules. When temperature increases, the additive melts and turns into liquid. Overall, it is concluded from these tests that the PET additive does not have much influence on the basic properties of bitumen binder.

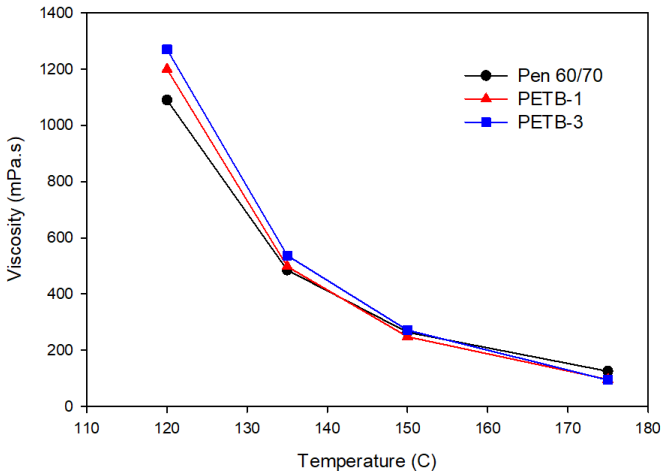

Figure 10. Viscosity measurement as a function of temperature

3.3 Boiling test

The images of the binder coated aggregate after the boiling tests were analyzed to compare the moisture susceptibility of PET additive modified asphalt binders. Figure 11 presents the original scanned images after boiling for 10 min and the corresponding binary images of the loose asphalt mixtures. The binary images were obtained through image analysis using MATLAB®, and the white area ratios representing the percentages of the stripped aggregates were computed [45] as shown in Figure 12. What stands out in the graph is that the boiling loss area for the control mixture was around 18.0%, which dropped considerably to around 10.0% with only 1wt% of PET additive. With further increasing of the PET additive dosage, the boiling loss area did not change much. As aforementioned, the PET additive may form crystal structures. When the concentration of PET additive increases, part of the additive can attract with each other and the amount of PET additive at the bitumen-aggregate interface may not change significantly. Therefore, the moisture susceptibility of the asphalt mixture can be effectively reduced with the incorporation of 1wt% of PET additive.

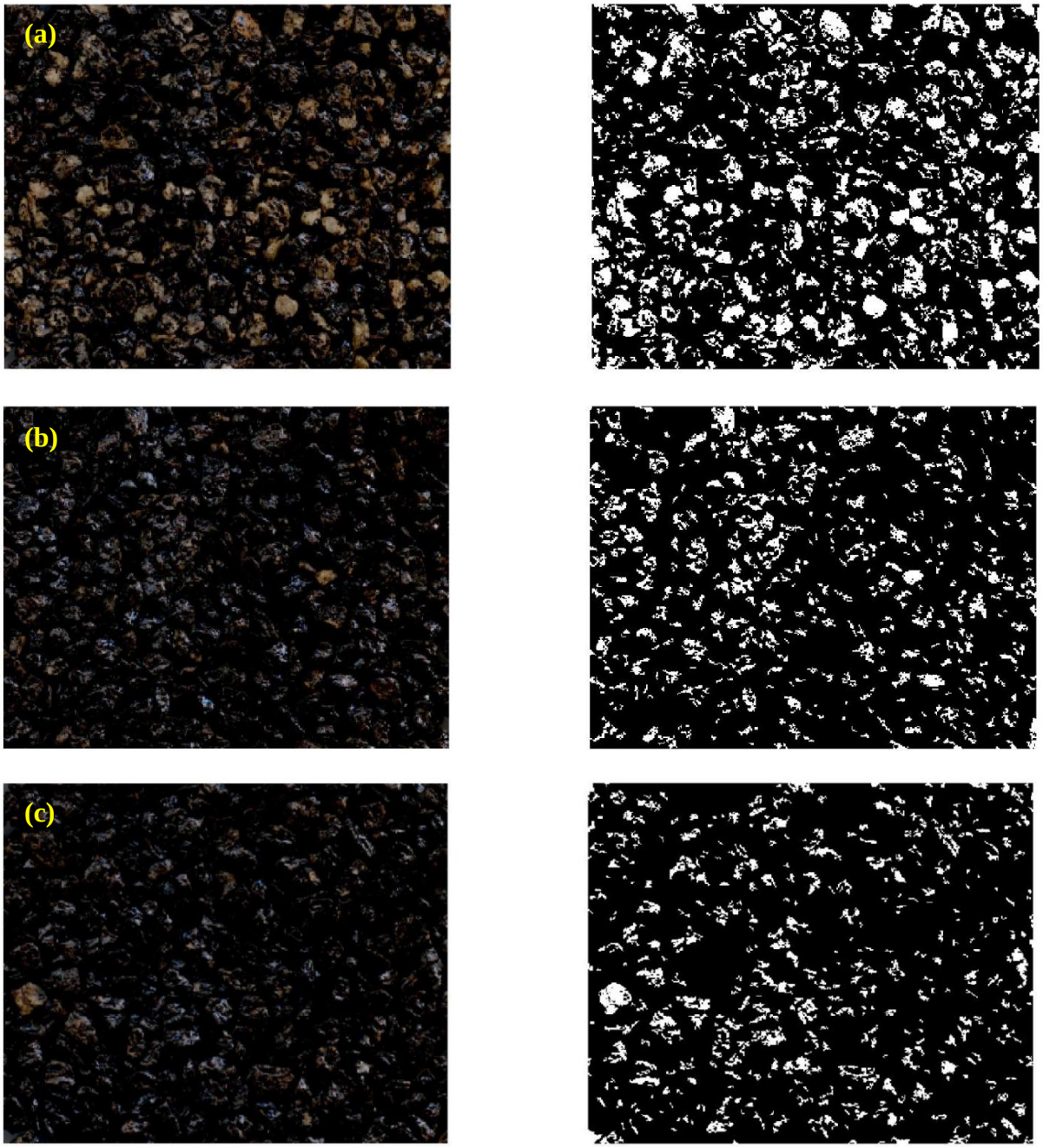

Figure 11. Original (left) and binary (right) images after boiling tests: (a) Pen 60/70, (b) PETB-1, and (c) PETB-3.

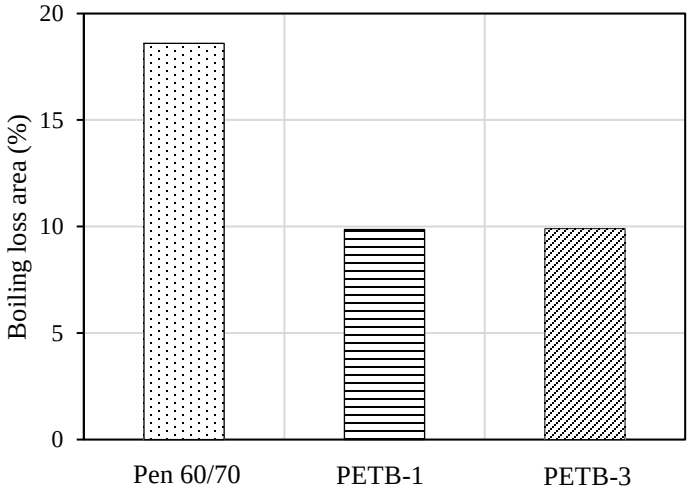

Figure 12. Comparison of boiling loss area.

3.4 ITS test

To further evaluate the effect of PET additive on the resistance to moisture-induced damage of asphalt mixture, the ITS tests were conducted on the compacted asphalt mixtures containing different dosages of PET additive. Figure 13 shows that the ITS values for the dry group were very close, around 1,000 kPa. However, after conditioning in water at 60℃ for 24 h, the ITS of the control asphalt mixture decreased sharply to 665.9 kPa, while there is no significant change in the wet conditioned ITS values for the PET modified asphalt mixtures. The TSR for the control asphalt mixture was around 60%, which increased dramatically to over 90% with the incorporation of only 1wt% of PET additive. With further increase of the PET additive dosage, the TSR did not change much. The fracture interface images of the samples in the wet-conditioned group after the ITS test are presented in Figure 14. It is clear that most of the Pen 60/70 bitumen was stripped off from the aggregate surface (Figure 14(a)), representing a distinct adhesive failure. However, no significant stripping was observed in the asphalt mixtures containing PET additive, indicating that the failure occurred within the bitumen binder or mastic phase, which is typically cohesive failure. Such

phenomenon indicated that the PET additive effectively increased the resistance to moisture-induced damage of asphalt mixture. The granite aggregate is acid, and the base bitumen binder is also acidic because of the presence of carboxylic and/or sulfonic groups [46]. Thus, the bonding between the granite aggregate and base bitumen binder is poor. The PET additive contains amine groups, which is an alkaline additive. The PET additive is expected to increase the bonding between the granite and bitumen binder for the following two reasons: 1) the amine groups in PET additive can form the strong hydrogen bonds with the hydroxyl groups at the aggregate surface, and 2) the alkaline amine groups can also increase the interaction between the granite aggregate and bitumen binder.

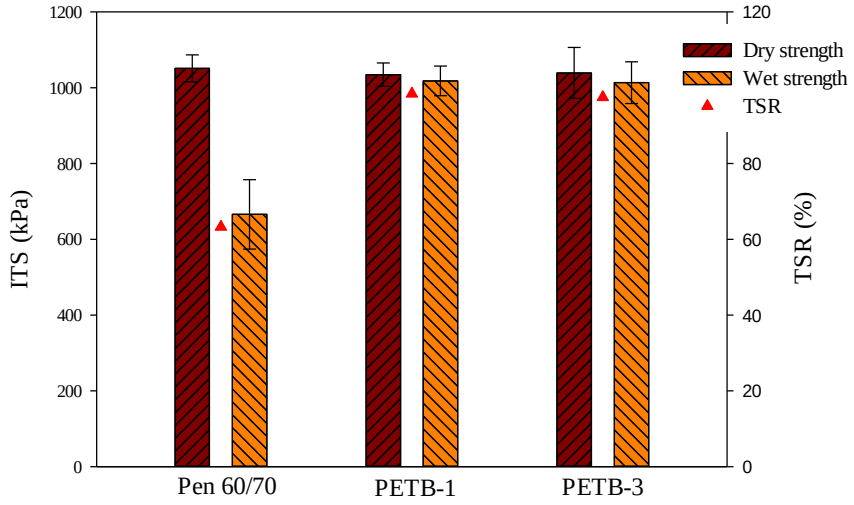

Figure 13. ITS of asphalt mixtures with different concentrations of PET additive at 20 °C (TSR represents the ratio between the wet tensile strength to the dry tensile strength).

Figure 14. Fracture interfaces for the asphalt mixtures that had been subjected to 24 h water conditioning at 60 °C: (a) Pen 60/70, (b) PETB-1, and (c) PETB-3.

4. MD simulation

4.1 Density

During the isothermal-isobaric (NPT) ensemble equilibration, the volume of the bitumen system decreased gradually, and the density increased accordingly. The density evolutions of the neat bitumen and PET additive modified bitumen (PETB) are shown in Figure 15. It can be seen that the densities of both neat bitumen and PETB increased sharply within the first 30 ps and then stabilized after 50 ps. Considering the low content of the PET additive, no significant difference was observed between the densities of the two binders. The equilibrated densities (averaged over the last 50 ps) of the neat bitumen and PETB are 0.906 g/cm^3 and 0.907 g/cm^3, respectively. The densities are consistent with those in the previous studies using the three-component bitumen model [24, 34].

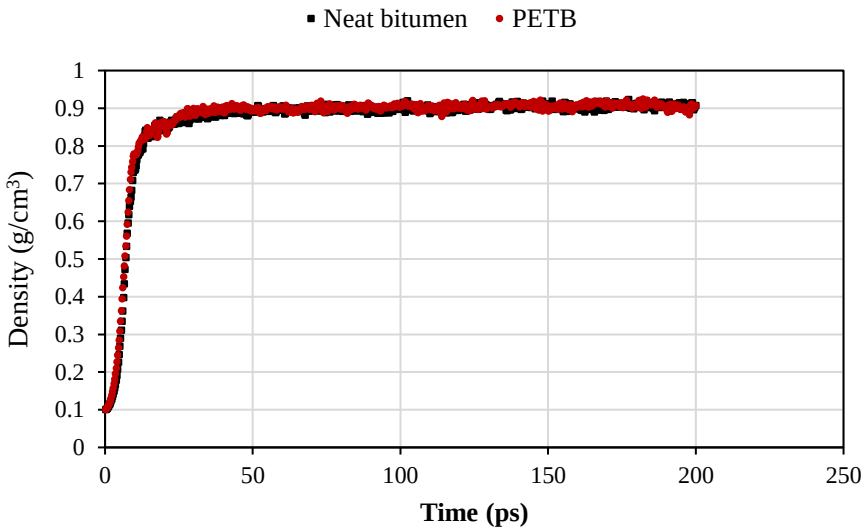

Figure 15. Densities of neat bitumen and PETB during equilibrium. The isothermal-isobaric (NPT) ensemble was implemented.

4.2. Cohesive energy density (CED) of binder

The cohesive energy density (CED) is used to quantify the magnitude of attraction between different molecules inside a substance. It is obtained from the difference of the total nonbond energy and the intramolecular nonbond energy, and the square root of CED is defined as the solubility parameter δ (Eq. (1)).

$$\delta = \sqrt{CED} \tag{1}$$

Table 4 presents the computed CED of the neat bitumen and PETB. With the incorporation of PET additive, the CED of PETB became larger than that of the neat bitumen, indicating that PET additive increased the molecular interaction. The result could be explained by that the PET additive is more polar than bitumen binder, thus both the van der Waals force and electrostatic force between different molecules increased, leading to stronger cohesion of PETB.

Table 4. Cohesive energy density (CED) of binder

Sample-ID	Van der Waals (10^6J/m^3)	Electrostatic (10^6J/m^3)	CED (10^6J/m^3)	Solubility Parameter ((J/cm^3)$^{0.5}$)
Neat bitumen	326.4	-1.221	332.4	18.232
PETB	334.5	0.610	342.6	18.509

Note: PETB represents the PET additive modified bitumen, in which 1 PET additive molecule was added into the bitumen model, corresponding to 1.97wt% of the PET additive based on bitumen.

4.3 Radial distribution

Figure 16 depicts the radial distribution of each component in the binder with respect to the aggregate surface. It can be seen that the concentration of 1,7-dimethylnaphthalene is the highest at the interface for the neat bitumen, followed by n-docosane and asphaltene. The first peak at

around 2 Å in Figure 16(b) belongs to the PET additive in PETB, indicating that the PET additive was the closest to the aggregate surface. As demonstrated in Figure 17, the amine groups in PET additive were very close to the aggregate surface. Two reasons may contribute to such phenomenon: (1) the higher polarity of PET additive makes it more affiliate to the polar aggregate surface, and (2) the amine groups in the PET additive and the hydroxyl groups in the aggregate surface can form hydrogen bond, which is much stronger compared with other non-bonded interactions.

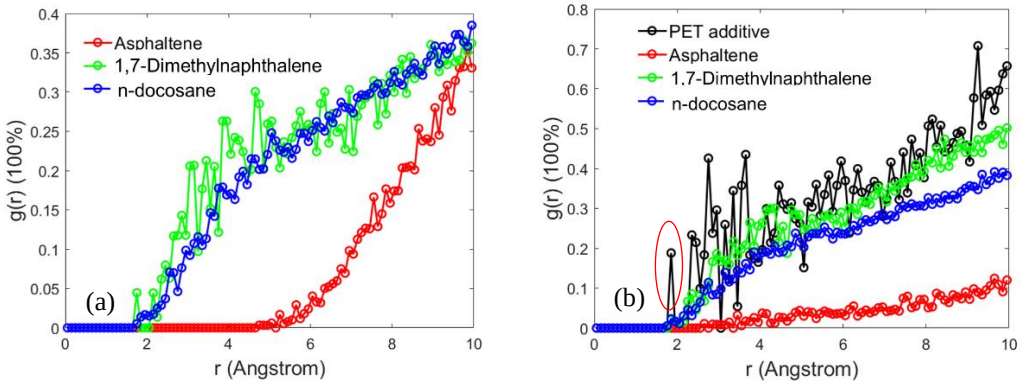

Figure 16. Radial distribution of each component respect to the aggregate surface: (a) neat bitumen; (b) PETB.

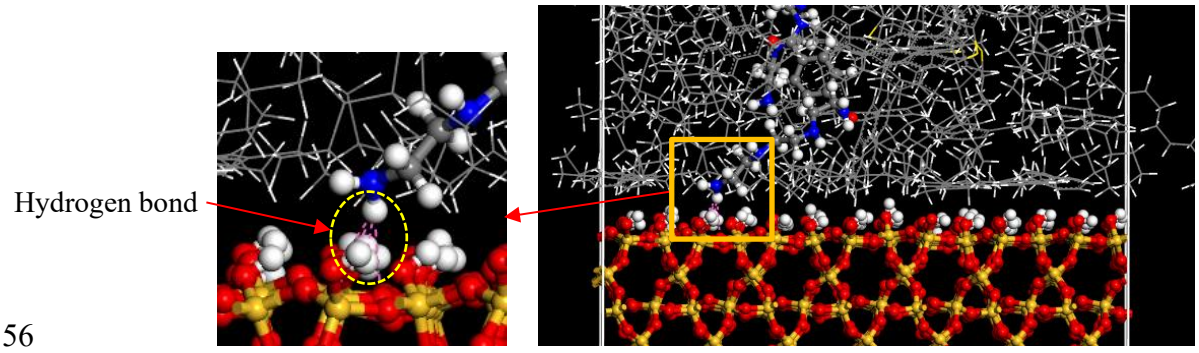

Figure 17. Interfacial interaction of PETB and aggregate.

4.4 Work of adhesion between binder and aggregate

The work of adhesion $W_{adhesion}$ is defined as the work required to separate the binder from aggregate at the interface, which determines the resistance to the interface detachment. A negative value of $W_{adhesion}$ indicates attraction of the two parts, whereas a positive value indicates repulsion. The work of adhesion $W_{adhesion}$ is given by Eq. (2), and the adhesion energy $\Delta E_{adhesion}$ is obtained from Eq. (3).

$$W_{adhesion} = \Delta E_{adhesion} / A \tag{2}$$

$$\Delta E_{adhesion} = E_{total} - (E_{binder} + E_{aggregate}) \tag{3}$$

where E_{total} is the total potential energy of the binder and aggregate interface system after equilibration, E_{binder} and $E_{aggregate}$ represent the potential energies of the binder and the aggregate separated at the equilibrium state, respectively, and A is the interface contact area.

Because of the hydrophilic nature of mineral aggregate, water is more likely to be absorbed onto the aggregate surface. As a result, asphalt binder is prone to detach from the aggregate in the presence of water. The adhesion energy $\Delta E_{adhesion\_water}$ and the work of adhesion $\Delta W_{adhesion\_water}$ in the presence of water are calculated using Eq. (4) and Eq. (5), respectively. A lower value of $\Delta E_{adhesion\_water}$ represents a lower energy potential for water to displace the binder from the aggregate surface [47], or the displacement is more difficult to happen and the resistance to moisture-induced damage is stronger.

$$\Delta E_{adhesion\_water} = \Delta E_{bit\_water} + \Delta E_{agg\_water} - \Delta E_{bit\_agg} \tag{4}$$

$$\Delta W_{adhesion\_water} = \Delta E_{adhesion\_water} / A \tag{5}$$

where ΔE_{bit_water} is the interaction energy between binder and water, ΔE_{agg_water} is the interaction energy between aggregate and water, and ΔE_{bit_agg} is the interaction energy between binder and aggregate. All the energies were obtained at the equilibrium state.

The energy ratio (ER), i.e., the ratio between the work of adhesion in dry condition and the work of adhesion in wet condition, is usually used to represent the moisture susceptibility of asphalt mixture [43, 47]. A larger value of ER indicates lower moisture sensitivity. The ER is given as,

$$ER = W_{adhesion} / W_{adhesion\_water} = \Delta E_{adhesion} / \Delta E_{adhesion\_water} \quad (6)$$

Table 5 shows the adhesion energy and work of adhesion between binder and aggregate in the dry condition. ΔE_{vdw} and ΔE_{elec} represent the energy difference associated with the van der Waals part and the electric part, respectively. Since both bitumen and aggregate possess high surface energy in isolated condition, when they attach to each other to form an interface, the total surface area becomes smaller, thus decreasing the potential energy of the system. This is the reason why the interaction energies in the table are negative. It is clear to see that the absolute value of the adhesion energy $\Delta E_{adhesion}$ and work of adhesion $W_{adhesion}$ for PETB and aggregate are larger than that of neat bitumen and aggregate, indicating that PET additive increased the interfacial adhesion between the binder and aggregate. Furthermore, it is observed that both the van der Waals and electric energy increased with the addition of PET additive. The increase of interface adhesion can be mainly attributed to the polarity of the PET additive and the formation of hydrogen bonding between the PET additive and aggregate surface hydroxyl groups.

Table 5. Adhesion energy of binder and aggregate in dry condition

Sample-ID	ΔE_{vdw} (kcal/mol)	ΔE_{elec} (kcal/mol)	$\Delta E_{adhesion}$ (kcal/mol)	$W_{adhesion}$ (mJ/m^2)
Agg_NB	-201.201	-1.897	-208.03	-118.03

Agg_PETB	-213.066	-8.658	-226.81	-128.68

Note: Agg_NB represents the interface between aggregate and neat bitumen in dry condition, and Agg_PETB represents the interface between aggregate and PET additive modified bitumen in dry condition.

Table 6 presents the adhesion energy in wet condition as well as the calculated energy ratio. It can be noticed that the absolute value of ΔE_{agg_water} is larger than that of ΔE_{bit_agg}, which demonstrates that water is more likely to be absorbed to the aggregate surface than bitumen binder due to the hydrophilic nature of the mineral aggregate. As shown in Table 6, the $\Delta E_{adhesion\_water}$ of the aggregate-water-PETB system is about 21% lower than that of the aggregate-water-NB system, indicating that the coating of PETB on the aggregate is harder to be replaced by water compared with neat bitumen. On the contrary, the ER of the PETB system reached 1.24, which is larger than that of the neat bitumen system (0.88). The simulation results revealed that the moisture sensitivity of the asphalt mixture was decreased by the incorporation of PET additive, which is consistent with the findings obtained from the preceding experiments.

Table 6. Adhesion energy of binder and aggregate in wet condition and the calculated ER

Sample-ID	ΔE_{bit_water} (kcal/mol)	ΔE_{agg_water} (kcal/mol)	ΔE_{bit_agg} (kcal/mol)	$\Delta E_{adhesion\_water}$ (kcal/mol)	ER
Agg_water_NB	-105.1	-200.0	-73.9	-231.3	0.88
Agg_water_PETB	-145.1	-158.3	-120.5	-182.9	1.24

Note: Agg_water_NB represents the interface between aggregate and neat bitumen in wet condition, and Agg_water_PETB represents the interface between aggregate and PET additive modified bitumen in wet condition.

5. Conclusions

In this study, the antistripping ability of the waste PET derived additive on asphalt mixture was investigated through both laboratory tests and MD simulation. The following points summarize the main conclusions of this study:

- The experimental results indicated that the boiling stripping area decreased significantly with the incorporation of PET additive. In addition, the TSR increased dramatically to over 90% with only 1wt% of PET additive, and the failure mode transferred from adhesive failure to cohesive failure.
- The MD simulation showed that PET additive improved the cohesive energy density of the binder.
- The adhesion between the binder and aggregate was strengthened by PET additive in both dry and wet condition. PET additive tends to approach the binder-aggregate interface, and form strong hydrogen bonding, thus increasing the interfacial adhesion. The higher polarity of PET additive in comparison with bitumen further increased the adhesion with the polar aggregate.

Both the experimental results and MD simulation indicated that the PET additive can improve the adhesion between asphalt binder and aggregate, thus increasing the resistance to moisture-induced damage of asphalt mixture. It is therefore concluded that the PET additive obtained from the aminolysis treated waste PET bottles can be successfully used as a sustainable antistripping agent in asphalt mixture. This technology transferred the waste PET into a value-added additive that is applicable in the pavement industry. In future studies, the effects of the PET derived antistripping additive on asphalt mixtures with different aggregates will be investigated, and the economic and

environmental performances of this technology will be evaluated through life cycle cost analysis and life cycle assessment, respectively.

Notes

The authors declare no competing financial interest.

Author Contributions

Rui Li: Conceptualization, Methodology, Experiments, Test result analysis, Manuscript drafting, Manuscript revision and editing. **Zhen Leng**: Conceptualization, Methodology, Test result analysis, Manuscript revision and editing. **Jun Yang**: Test result analysis, Manuscript revision and editing. **Guoyang Lu**: Test result analysis, Manuscript revision and editing. **Man Huang**: Test result analysis, Manuscript revision and editing. **Jingting Lan:** Experiments, Test result analysis. **Hongliang Zhang**: Test result analysis. **Yawei Bai:** Test result analysis, Manuscript revision. **Zejiao Dong:** Test result analysis, Manuscript revision.

Funding Sources

The authors would like to acknowledge the funding support from the Hong Kong Environment and Conservation Fund through ECF Project 84/2017 and Science and Technology Project of Henan Provincial Department of Transportation (Project number: 2020J6).

Acknowledgment

The authors would like to acknowledge the insightful discussions about molecular dynamics simulation with Dr. Yangming Gao from Aston University in UK and Dr. Chi Zhang from ETH in Switzerland.

Appendix

The COMPASS force field, developed using *ab initio* and empirical parameterization techniques by Sun [37], can well describe the interactions of both organic and inorganic materials. Previous studies [38, 39] have successfully applied the COMPASS force field to simulate the bitumen and aggregate. The total potential energy of COMPASS force field constitutes the valence energy (E_{val}, *bonded*) and non-bonded energy ($E_{non\text{-}bond}$),

$$E_{total} = E_{val} + E_{non-bond}$$

The valence energy is composed by,

$$E_{val} = E_b + E_\theta + E_\varphi + E_\chi + E_{bb'} + E_{b\theta} + E_{b\varphi} + E_{\theta\varphi} + E_{\theta\theta'} + E_{\theta\theta'\varphi}$$

in which E_b, E_θ, E_φ, and E_χ, represent the bond stretching, angle bending, internal torsion, and out-of-plane bending terms, respectively, and $E_{bb'}$, $E_{b\theta}$, $E_{b\varphi}$, $E_{\theta\varphi}$, $E_{\theta\theta'}$, $E_{\theta\theta'\varphi}$ stand for cross-coupling terms between two or three internal coordinates.

More detailly, these valence terms are described as follow,

$$E_b = \sum_b [k_2 (b - b_0)^2 + k_3 (b - b_0)^3 + k_4 (b - b_0)^4]$$

$$E_\theta = \sum_\theta [k_2 (\theta - \theta_0)^2 + k_3 (\theta - \theta_0)^3 + k_4 (\theta - \theta_0)^4]$$

$$E_\varphi = \sum_\varphi [k_1 (1 - \cos\varphi) + k_2 (1 - \cos 2\varphi) + k_3 (1 - \cos 3\varphi)]$$

$$E_\chi = \sum_\chi k_2 \chi^2$$

$$E_{bb'} = \sum_{b,b'} k(b - b_0)(b' - b_0')$$

$$E_{b\theta} = \sum_{b,\theta} k(b - b_0)(\theta - \theta_0)$$

$$E_{b\varphi} = \sum_{b,\varphi} (b - b_0)(k_1 \cos\varphi + k_2 \cos 2\varphi + k_3 \cos 3\varphi)$$

$$E_{\theta\varphi} = \sum_{\theta,\varphi} (\theta - \theta_0)(k_1 \cos\varphi + k_2 \cos 2\varphi + k_3 \cos 3\varphi)$$

$$E_{\theta\theta'} = \sum_{\theta,\theta'} k(\theta - \theta_0)(\theta' - \theta_0')$$

$$E_{\theta\theta'\varphi} = \sum_{\theta,\theta',\varphi} k(\theta - \theta_0)(\theta' - \theta_0')\cos\varphi$$

The non-bonded interaction includes the Coulomb electrostatic energy (E_{elec}) and van der Waals (E_{vdW}) energy,

$$E_{non-bond} = E_{elec} + E_{vdW}$$

and they are described as,

$$E_{elec} = \sum_{i,j} \frac{q_i q_j}{r_{ij}}$$

$$E_{vdW} = \sum_{i,j} \varepsilon_{ij} \left[2\left(\frac{r_{ij}^0}{r_{ij}}\right)^9 - 3\left(\frac{r_{ij}^0}{r_{ij}}\right)^6 \right]$$

The simulation details are presented in Table a1.

Table a1 Simulation details

Bulk bitumen binder model							
Procedure	Timestep (fs)	Duration (ps)	Ensemble	Temperature (K)	Pressure (GPa)	Thermostat	Barostat
Anneal	1	5	NVT	300-500 (5 cycles)	/	NHL	/
Pre-equilibrium	1	100	NVT	298	/	NHL	/
Equilibrium	1	200	NPT	298	0.0001	NHL	Andersen
Final equilibrium	1	100	NVT	298	/	NHL	/
Bitumen-aggregate interface model							
Equilibrium	1	200	NVT	298	/	NHL	/

Note: NHL represents the Nose-Hoover-Langevin thermostat.

References

[1] A. Collop, Y. Choi, G. Airey, and R. Elliott, "Development of the saturation ageing tensile stiffness (SATS) test," in *Proceedings of the Institution of Civil Engineers-Transport*, 2004, vol. 157, no. 3, pp. 163-171: Thomas Telford Ltd.

[2] J. Emery and H. Seddik, *Moisture damage of asphalt pavements and antistripping additives: Causes, identification, testing and mitigation*. 1997.

[3] G. D. Airey and Y.-K. Choi, State of the Art Report on Moisture Sensitivity Test Methods for Bituminous Pavement Materials, *Road Materials and Pavement Design,* vol. 3, no. 4, pp. 355-372, 2002/01/01 2002.

[4] R. Gubler, M. Partl, F. Canestrari, and A. Grilli, Influence of water and temperature on mechanical properties of selected asphalt pavements, *Materials and structures,* vol. 38, no. 5, pp. 523-532, 2005.

[5] J. Grenfell, N. Ahmad, Y. Liu, A. Apeagyei, D. Large, and G. Airey, Assessing asphalt mixture moisture susceptibility through intrinsic adhesion, bitumen stripping and mechanical damage, *Road Materials and Pavement Design,* vol. 15, no. 1, pp. 131-152, 2014.

[6] Y. Liu, A. Apeagyei, N. Ahmad, J. Grenfell, and G. Airey, Examination of moisture sensitivity of aggregate–bitumen bonding strength using loose asphalt mixture and physico-chemical surface energy property tests, *International Journal of Pavement Engineering,* vol. 15, no. 7, pp. 657-670, 2014/08/09 2014.

[7] D. Cheng, D. N. Little, R. L. Lytton, and J. C. Holste, Surface Energy Measurement of Asphalt and Its Application to Predicting Fatigue and Healing in Asphalt Mixtures, *Transportation Research Record,* vol. 1810, no. 1, pp. 44-53, 2002/01/01 2002.

[8] P. S. Kandhal, Field and Laboratory Evaluation of Stripping in Asphalt Pavements, *Transportation Research Record,* vol. 1454, 1994.

[9] H. J. Fromm, The mechanisms of asphalt stripping from aggregate surfaces, *Proceedings of the Association of Asphalt Paving Technologis,* vol. 43, 1974.

[10] M. Nazirizad, A. Kavussi, and A. Abdi, Evaluation of the effects of anti-stripping agents on the performance of asphalt mixtures, *Construction and Building Materials,* vol. 84, pp. 348-353, 2015.

[11] P. E. Sebaaly, D. Little, E. Y. Hajj, and A. Bhasin, Impact of Lime and Liquid Antistrip Agents on Properties of Idaho Hot-Mix Asphalt Mixture, *Transportation Research Record,* vol. 1998, no. 1, pp. 65-74, 2007/01/01 2007.

[12] E. Hesami and G. Mehdizadeh, Study of the amine-based liquid anti-stripping agents by simulating hot mix asphalt plant production process, *Construction and Building Materials,* vol. 157, pp. 1011-1017, 2017.

[13] D.-W. Park, W.-J. Seo, J. Kim, and H. V. Vo, Evaluation of moisture susceptibility of asphalt mixture using liquid anti-stripping agents, *Construction and Building Materials,* vol. 144, pp. 399-405, 2017.

[14] E. Iskender, A. Aksoy, and H. Ozen, Indirect performance comparison for styrene–butadiene–styrene polymer and fatty amine anti-strip modified asphalt mixtures, *Construction and building materials,* vol. 30, pp. 117-124, 2012.

[15] A. Aksoy, K. Şamlioglu, S. Tayfur, and H. Özen, Effects of various additives on the moisture damage sensitivity of asphalt mixtures, *Construction and Building Materials,* vol. 19, no. 1, pp. 11-18, 2005.

[16] A. Modarres and H. Hamedi, Developing laboratory fatigue and resilient modulus models for modified asphalt mixes with waste plastic bottles (PET), *Construction and Building Materials,* vol. 68, pp. 259-267, 2014.
[17] A. Modarres and H. Hamedi, Effect of waste plastic bottles on the stiffness and fatigue properties of modified asphalt mixes, *Materials and Design,* vol. 61, pp. 8-15, 2014.
[18] T. B. Moghaddam, M. R. Karim, and T. Syammaun, Dynamic properties of stone mastic asphalt mixtures containing waste plastic bottles, *Construction and Building Materials,* vol. 34, pp. 236-242, 2012.
[19] E. Ahmadinia, M. Zargar, M. R. Karim, M. Abdelaziz, and E. Ahmadinia, Performance evaluation of utilization of waste Polyethylene Terephthalate (PET) in stone mastic asphalt, *Construction and Building Materials,* vol. 36, pp. 984-989, 2012.
[20] Z. Leng, A. Sreeram, R. K. Padhan, and Z. Tan, Value-added application of waste PET based additives in bituminous mixtures containing high percentage of reclaimed asphalt pavement (RAP), *Journal of Cleaner Production,* vol. 196, pp. 615-625, 2018/09/20/ 2018.
[21] H. Zhang, M. Huang, J. Hong, F. Lai, and Y. Gao, Molecular dynamics study on improvement effect of bis(2-hydroxyethyl) terephthalate on adhesive properties of asphalt-aggregate interface, *Fuel,* vol. 285, p. 119175, 2021/02/01/ 2021.
[22] D. R. Merkel *et al.*, Waste PET Chemical Processing to Terephthalic Amides and Their Effect on Asphalt Performance, *ACS Sustainable Chemistry & Engineering,* vol. 8, no. 14, pp. 5615-5625, 2020/04/13 2020.
[23] Z. Leng, R. K. Padhan, and A. Sreeram, Production of a sustainable paving material through chemical recycling of waste PET into crumb rubber modified asphalt, *Journal of cleaner production,* vol. 180, pp. 682-688, 2018.
[24] G. Xu and H. Wang, Study of cohesion and adhesion properties of asphalt concrete with molecular dynamics simulation, *Computational Materials Science,* vol. 112, pp. 161-169, 2016/02/01/ 2016.
[25] M. Xu, J. Yi, D. Feng, Y. Huang, and D. Wang, Analysis of Adhesive Characteristics of Asphalt Based on Atomic Force Microscopy and Molecular Dynamics Simulation, *ACS Applied Materials & Interfaces,* vol. 8, no. 19, pp. 12393-12403, 2016/05/18 2016.
[26] L. Zhang and M. L. Greenfield, Relaxation time, diffusion, and viscosity analysis of model asphalt systems using molecular simulation, *The Journal of Chemical Physics,* vol. 127, no. 19, p. 194502, 2007.
[27] Y. Lu and L. Wang, Nano-mechanics modelling of deformation and failure behaviours at asphalt–aggregate interfaces, *International Journal of Pavement Engineering,* vol. 12, no. 4, pp. 311-323, 2011/08/01 2011.
[28] A. Bhasin, R. Bommavaram, M. L. Greenfield, and D. N. Little, Use of Molecular Dynamics to Investigate Self-Healing Mechanisms in Asphalt Binders, *Journal of Materials in Civil Engineering,* vol. 23, no. 4, pp. 485-492, 2011.
[29] H. Yao, Q. Dai, and Z. You, Chemo-physical analysis and molecular dynamics (MD) simulation of moisture susceptibility of nano hydrated lime modified asphalt mixtures, *Construction and Building Materials,* vol. 101, pp. 536-547, 2015/12/30/ 2015.
[30] C. Ling, R. Moraes, D. Swiertz, and H. Bahia, Measuring the Influence of Aggregate Coating on the Workability and Moisture Susceptibility of Cold-Mix Asphalt, *Transportation Research Record,* vol. 2372, no. 1, pp. 46-52, 2013/01/01 2013.

[31] L. W. Corbett, Composition of asphalt based on generic fractionation, using solvent deasphaltening, elution-adsorption chromatography, and densimetric characterization, *Analytical Chemistry,* vol. 41, no. 4, pp. 576-579, 1969/04/01 1969.
[32] M. L. Greenfield and L. Zhang, "Developing model asphalt systems using molecular simulation: final model," University of Rhode Island. Transportation Center2009.
[33] D. D. Li and M. L. Greenfield, Chemical compositions of improved model asphalt systems for molecular simulations, *Fuel,* vol. 115, pp. 347-356, 2014/01/01/ 2014.
[34] L. Zhang and M. L. Greenfield, Analyzing Properties of Model Asphalts Using Molecular Simulation, *Energy & Fuels,* vol. 21, no. 3, pp. 1712-1716, 2007/05/01 2007.
[35] Y. Ding, B. Huang, X. Shu, Y. Zhang, and M. E. Woods, Use of molecular dynamics to investigate diffusion between virgin and aged asphalt binders, *Fuel,* vol. 174, pp. 267-273, 2016/06/15/ 2016.
[36] H. Yao, Q. Dai, and Z. You, Molecular dynamics simulation of physicochemical properties of the asphalt model, *Fuel,* vol. 164, pp. 83-93, 2016/01/15/ 2016.
[37] H. Sun, COMPASS: An ab Initio Force-Field Optimized for Condensed-Phase ApplicationsOverview with Details on Alkane and Benzene Compounds, *The Journal of Physical Chemistry B,* vol. 102, no. 38, pp. 7338-7364, 1998/09/01 1998.
[38] Y. Gao, Y. Zhang, F. Gu, T. Xu, and H. Wang, Impact of minerals and water on bitumen-mineral adhesion and debonding behaviours using molecular dynamics simulations, *Construction and Building Materials,* vol. 171, pp. 214-222, 2018/05/20/ 2018.
[39] Z. Dong, Z. Liu, P. Wang, and X. Gong, Nanostructure characterization of asphalt-aggregate interface through molecular dynamics simulation and atomic force microscopy, *Fuel,* vol. 189, pp. 155-163, 2017/02/01/ 2017.
[40] W. Ding, H. Jin, Q. Zhao, B. Chen, and W. Cao, Dissolution of polycyclic aromatic hydrocarbons in supercritical water in hydrogen production process: A molecular dynamics simulation study, *International Journal of Hydrogen Energy,* vol. 45, no. 52, pp. 28062-28069, 2020/10/23/ 2020.
[41] H. H. Yoon and A. R. Tarrer, *Effect of aggregate properties on stripping* (no. 1171). Transportation Research Record, 1988.
[42] L. T. Zhuravlev, Concentration of hydroxyl groups on the surface of amorphous silicas, *Langmuir,* vol. 3, no. 3, pp. 316-318, 1987/05/01 1987.
[43] G. Xu and H. Wang, Molecular dynamics study of interfacial mechanical behavior between asphalt binder and mineral aggregate, *Construction and Building Materials,* vol. 121, pp. 246-254, 2016/09/15/ 2016.
[44] Y. Gao, Y. Zhang, Y. Yang, J. Zhang, and F. Gu, Molecular dynamics investigation of interfacial adhesion between oxidised bitumen and mineral surfaces, *Applied Surface Science,* vol. 479, pp. 449-462, 2019/06/15/ 2019.
[45] C. Ling, A. Hanz, and H. Bahia, Measuring moisture susceptibility of Cold Mix Asphalt with a modified boiling test based on digital imaging, *Construction and Building Materials,* vol. 105, pp. 391-399, 2016.
[46] A. Jada and M. Salou, Effects of the asphaltene and resin contents of the bitumens on the water–bitumen interface properties, *Journal of Petroleum Science and Engineering,* vol. 33, no. 1, pp. 185-193, 2002/04/01/ 2002.
[47] A. Bhasin, J. Howson, E. Masad, D. N. Little, and R. L. Lytton, Effect of Modification Processes on Bond Energy of Asphalt Binders, *Transportation Research Record,* vol. 1998, no. 1, pp. 29-37, 2007.

627